Atmospheric Environment 147 (2016) 446–457

Contents lists available at ScienceDirect

Atmospheric Environment

journal homepage: www.elsevier.com/locate/atmosenv

Calibrating R-LINE model results with observational data to develop annual mobile source air pollutant fields at fine spatial resolution: Application in Atlanta

Xinxin Zhai [a], Armistead G. Russell [a], Poornima Sampath [a], James A. Mulholland [a, *], Byeong-Uk Kim [b], Yunhee Kim [b], David D'Onofrio [c]

[a] Georgia Institute of Technology, United States
[b] Georgia Environmental Protection Division, United States
[c] Atlanta Regional Commission, United States

HIGHLIGHTS

- An approach is developed using the R-LINE dispersion model to calculate annual average mobile source air pollutant metrics.
- A method is developed to calibrate R-LINE estimates to observations and to CMB-GC estimated mobile source impacts.
- Higher exposures are found using calibrated R-LINE fields than using fields from coarse resolution regional scale models.

ARTICLE INFO

Article history:
Received 28 July 2016
Received in revised form
20 September 2016
Accepted 7 October 2016
Available online 11 October 2016

Keywords:
Air quality
R-LINE
Dispersion model
CMB-GC

ABSTRACT

The Research LINE-source (R-LINE) dispersion model for near-surface releases is a dispersion model developed to estimate the impacts of line sources, such as automobiles, on primary air pollutant levels. In a multiyear application in Atlanta, R-LINE simulations overestimated concentrations and spatial gradients compared to measurements. In this study we present a computationally efficient procedure for calculating annual average spatial fields and develop an approach for calibrating R-LINE concentrations with observational data. Simulated hourly concentrations of $PM_{2.5}$, CO and NO_x from mobile sources at 250 m resolution in the 20-county Atlanta area based on average diurnal emission profiles and meteorological categories were used to estimate annual averages. Compared to mobile source $PM_{2.5}$ impacts estimated by chemical mass balance with gas constraints (CMB-GC), a source apportionment model based on $PM_{2.5}$ speciation measurements, R-LINE estimates of traffic-generated $PM_{2.5}$ impacts were found to be higher by a factor of 1.8 on average across all sites. Compared to observations of daily 1 h maximum CO and NO_x, R-LINE estimates were higher by factors of 1.3 and 4.2 on average, respectively. Annual averages estimated by R-LINE were calibrated by regression with observations from 2002 to 2011 at multiple sites for daily 1 h maximum CO and NO_x and with measurement-based mobile source impacts estimated by CMB-GC for $PM_{2.5}$. The calibration reduced normalized mean bias (NMB) from 29% to 0.3% for $PM_{2.5}$, from 22% to −1% for CO, and from 303% to 49% for NO_x. Cross-validation analysis (withholding sites one at a time) leads to NMB of 13%, 1%, and 69% for $PM_{2.5}$, CO, and NO_x, respectively. The observation-calibrated R-LINE annual average spatial fields were compared with pollutant fields from observation-blended, 12 km resolution Community Multi-scale Air Quality (CMAQ) model fields for CO and NO_x, with Pearson correlation R^2 values of 0.55 for CO and 0.54 for NO_x found. The calibrated fields of $PM_{2.5}$ were compared with 4 km resolution mobile source impact fields obtained from an indicator method using the observation-CMAQ fields, with an R^2 value of 0.53 found. The method developed provides high-resolution annual average spatial fields in a computationally efficient manner with low bias. The method is being applied in air quality planning efforts and the pollutant concentration fields are being used in long-term, fine spatial scale health studies.

* Corresponding author.
E-mail address: james.mulholland@ce.gatech.edu (J.A. Mulholland).

http://dx.doi.org/10.1016/j.atmosenv.2016.10.015

1. Introduction

Traffic is a major source of ambient air pollution, including fine particulate matter ($PM_{2.5}$), carbon monoxide (CO), and nitrogen oxides (NO_x). Both long-term and short-term exposures to traffic-generated air pollutants are associated with adverse health effects such as cardiovascular disease, impaired lung development, and respiratory disease (Brook et al., 2010; Gauderman et al., 2007; Lim et al., 2012; Nordling et al., 2008). With 19% of the United States population living close to roads with heavy traffic, the health burden of exposure to traffic-related pollutants is potentially significant (Rowangould, 2013). As a result, pollutant monitors have been located near roadways (Chen et al., 2013; Environmental Protection Agency, 2009). Assessing exposure to traffic-related pollution is difficult, however, due to the steep, non-linear concentration gradients near roads. Distance to roadway is often used as a surrogate for traffic pollution exposure in health studies (Jerrett et al., 2005). New methods are warranted to provide improved traffic-concentration-exposure relationships for use in health studies.

Ambient measurements and model simulations have been used to assess exposures to traffic-related air pollutants, but both have their limitations. The major issue associated with using measurements is the sparse ambient air monitor network that severely limits the spatial representativeness of exposure estimates. While near-road monitoring does exist (Environmental Protection Agency, 2009; 2011; Reche et al., 2011), the network is very limited with single monitors in a few urban areas. Spatial concentration gradients are difficult to capture and generalize to other areas. Further, it is not directly apparent what fraction of the pollutants measured at a monitoring site comes from mobile sources. Air quality models can be used to help address these limitations by simulating spatial and temporal distributions of traffic-related pollution. Air quality models use emissions from sources and meteorological conditions to simulate traffic impacts, typically at the hourly level, over a range of spatial scales. Over regional and global domains, chemical transport models (CTMs) are used to capture large-scale pollutant transport, transformation, and fate, including both primary pollutants emitted directly from sources and secondary species formed in the atmosphere such as ozone and secondary organic aerosol (Baldassarre et al., 2015; Ivey et al., 2015; Liu et al., 2010; Wang et al., 2010). Due in part to the parameterizations used and computational requirements, CTM approaches typically have spatial resolutions of 4 km or more and, therefore, miss the fine scale gradients of primary pollutants.

For city-level simulations, dispersion models can be used to simulate concentrations of primary pollutants at finer resolutions (Chang et al., 2015; Gulliver and Briggs, 2011; Jerrett et al., 2005; Venkatram et al., 2007). Such models are typically based on solving a simplified form of the pollutant transport equation (e.g., Gaussian models such as the Industrial Source Complex (ISC) model (Bowers et al., 1980)) and have limited descriptions of chemical transformation. Two of the more advanced and widely used dispersion models are the American Meteorological Society (AMS) and Environmental Protection agency (EPA) Regulatory Model (AERMOD) (Cimorelli et al., 2005) frequently used for stationary sources including industries, and the Research LINE-source dispersion model for near-surface releases (R-LINE) (Snyder et al., 2013). R-LINE is a steady-state plume model used in support of evaluating the exposures to near-traffic environments. It is specifically designed for line sources and is formulated with a new plume meandering algorithm for light wind conditions (Snyder et al., 2013; Venkatram et al., 2013). However, previous research found that dispersion models in general over-estimate the pollutant concentrations (Venkatram et al., 2004).

The biased results from emission-based models are being increasingly calibrated to receptor-based observations, as formulated in data blending and data assimilation methods (Crooks and Ozkaynak, 2014; Friberg et al., 2016; Wilton et al., 2010). Such calibration procedures have long been used in more statistical approaches, such as satellite data models and land-use regression models (LUR) (Beckerman et al., 2013; Lv et al., 2016). Land-use regression models are widely used for estimating fine-scale air pollution metrics (Arain et al., 2007; Hankey and Marshall, 2015; Wang et al., 2016). LUR models predict fine-scaled and area-specific air pollution fields utilizing predictor variables such as traffic information, population distribution, land use, and meteorology conditions (including, in some cases, wind speed and direction). Typically, LUR models capture the spatial distribution of annual average levels over urban areas. However, LUR model applications are limited to the area in which they are developed (Hoek et al., 2008).

In this study we use R-LINE model to develop 10 years of annual average fields for mobile source-derived $PM_{2.5}$, daily 1 h maximum CO, and daily 1 h maximum NO_x in the Atlanta metropolitan region. These metrics align with the National Ambient Air Quality Standards (NAAQS) (United States, 1990) and the 1 h maximum values are commonly used as surrogate of NO_x and CO pollution in regional planning and health study applications (NAAQS is for NO_2 while we used NO_x). We use a regression approach to calibrate R-LINE model results to observations and to mobile source impacts estimated from observational data, and evaluate results using data withholding. Finally, the bias-corrected fine resolution R-LINE results are compared with regional scale fields derived using previously developed methods (Friberg et al., 2016; Pachon et al., 2012).

2. Methods

Methods used in this work are described in three parts. First, R-LINE is applied to estimate annual concentrations of $PM_{2.5}$, CO, and NO_x from mobile sources in the Atlanta, GA, 20-county metropolitan area at 250 m resolution for 2002 to 2011. An approach was developed for calculating annual averages based on the application of STability ARray (STAR) method to dispersion models (Chang et al., 2015; D'Onofrio et al., 2016; Environmental Protection Agency, 1997) and adjusted with emission diurnal trends. Second, to reduce bias, these fields are calibrated using a regression model approach with ten years of observations for CO and NO_x at five and seven sites, respectively, and, in the case of mobile source $PM_{2.5}$, with ten years of estimates at three locations with speciated $PM_{2.5}$ measurements obtained via the receptor-based source apportionment Chemical Mass Balance Method with Gas Constraints (CMB-GC) (Environmental Protection Agency, 2004a; Marmur et al., 2005). Cross validation by data withholding is performed to further evaluate the effectiveness of the calibration and the limitation of the number of monitors. Third, the resulting calibrated fields are then compared to fields at coarser resolution obtained from simulations with the Community Multi-Scale Air Quality (CMAQ) (Byun et al., 1997) blended with observations (Friberg et al., 2016) by aggregating to the CMAQ grid (as described later).

2.1. R-LINE dispersion model

The R-LINE model is a steady-state dispersion model for line sources (Snyder et al., 2013). It simulates physical dispersion processes but not chemical processes, so is applicable for primary and chemically inert pollutants. It takes inputs such as wind speed, wind direction, Monin-Obukhov length for turbulence, surface friction velocity, and other meteorological parameters, but does not consider the impact of wet deposition (e.g., due to precipitation) or

non-linear chemical transformation (Venkatram et al., 2013). In this research, we use annual average pollutant concentrations for evaluation, which are less impacted than hourly results by the lack of a wet deposition sink. The domain is the 20-county Atlanta metropolitan region. R-LINE simulates line-source emissions (described below) as point sources along a line and calculates steady state concentrations by solving Gaussian dispersion equations. It provides two options: a numerical integration approach and an approximate analytical solution (Environmental Protection Agency, 2013). Here we adopt the numerical approach and calculate annual average concentrations for ten years at multiple monitor locations (three for $PM_{2.5}$, five for CO, and seven for NO_x) for use in calibration, and at 250 m resolution (235,296 spatial locations) for use in spatial field development.

2.1.1. Meteorological inputs

Hourly meteorological data for 2002 to 2011 are generated using AERMET (Cimorelli et al., 2005; Environmental Protection Agency, 2004b) and AERMINUTE (Environmental Protection Agency, 2015), the meteorological processors of AERMOD. Surface meteorological data are from the National Weather Service (NWS) at the Hartsfield-Jackson International Airport. We use AERMINUTE (Version 15272) to process 1-min wind speed and wind direction data from the Automated Surface Observing Stations (ASOS) (http://www.nws.noaa.gov/ost/asostech.html) to reduce the number of calms and missing wind data in the hourly surface data. AERMET (Version 15181) processes hourly surface friction velocity, convective scale, Monin-Obukhov length, and surface roughness height within the surface layer. The missing hours (0.025% of the total for 2002 to 2011) are not included in the calculation, and meet the data completeness by requirements of EPA policy (more than 90% available) (Environmental Protection Agency, 2000).

2.1.2. Emission inputs

Emission inputs to R-LINE are 2010 link emissions based on Atlanta Regional Commission's (ARC) 20-county activity-based travel demand model and scaled to annual average levels for other years. Hourly emissions for 2010 at 43,712 links were generated for CO, NO_x and primary $PM_{2.5}$ over the 20-county regional area; 24 h average emission data are shown in Fig. 1 for $PM_{2.5}$, CO, and NO_x. Hourly emission rates for 24 h (assumed to be an average weekday) were generated for the Atlanta Roadside Emissions Exposure Study (AREES) by ARC with the purpose of understanding traffic impacts on air quality in Atlanta. Local traffic emissions are based on the link-level information, including road type and location, traffic volume, and vehicle type and speed. Emission factors are developed using the Motor Vehicle Emission Simulator 2010b (MOVES2010b) (Environmental Protection Agency, 2012) using a 2010 base year with Atlanta traffic volume and speed and vehicle fleet composition information. Relative emissions for the three species differ spatially because of the patterns of diesel and gasoline vehicles. As more CO emissions are contributed by gasoline vehicles and more elemental carbon emissions in $PM_{2.5}$ are contributed by diesel vehicles (Lena et al., 2001; Parrish, 2006), relatively greater CO emissions are observed in the center of the city because pass-through truck traffic is limited on freeways inside the interstate highway (I-285) circling Atlanta.

2.1.3. Annual average approach

The STAR approach was developed for computational efficiency by grouping the frequency distribution of wind speed, wind direction, and stability (Environmental Protection Agency 1997), and has been applied to estimate annual mean fields (Chang et al., 2015; D'Onofrio et al., 2016). An annual averaging approach was developed here based on the application of STAR as well as diurnal emission profiles as described below (Fig. S1).

First, low wind speeds ("calm conditions", (Environmental Protection Agency, 2000)) were treated by setting a minimum wind velocity of 1 m/s (see SI and Fig. S2 for discussion and analysis) to minimize unrealistically high simulated concentrations. Second, meteorological conditions are categorized for input to R-LINE. In this application, we chose Monin-Obukhov length, wind direction, and wind speed. We defined 80 categories based on these three parameters, with five levels of stability conditions defined by Monin-Obukhov length ranges, four wind directions, and four wind speed ranges (Table 1). Over the 10-year study period (2002–2011), 78 out of the 80 categories were observed.

Third, we assume a consistent roadway link pattern and vehicle type distribution over time. Annual trends were based on total emissions of the 20-county region in Atlanta estimated by MOVES and are shown normalized to 2010 emissions in Fig. 2a. We define an annual average emission ratio ($\overline{ER_j}$) as the ratio of year j emissions vs 2010 emissions in the 20-county area calculated using MOVES (Table S1). Link emissions for each year are the 2010 emissions multiplied by $\overline{ER_j}$ (Fig. 2a). The annual emissions decrease over the ten-year period by a factor of 1.8, 1.5, and 2.0 for $PM_{2.5}$, CO, and NO_x, respectively (Fig. 2a).

The 24 h diurnal trend was scaled using emission ratios as well. With the diurnal emission pattern (24 h) and 80 meteorological bins, there are 1920 conditions for each year. Since R-LINE calculated concentrations are proportional to emissions (Venkatram et al., 2013), and the spatial distributions of emissions for each

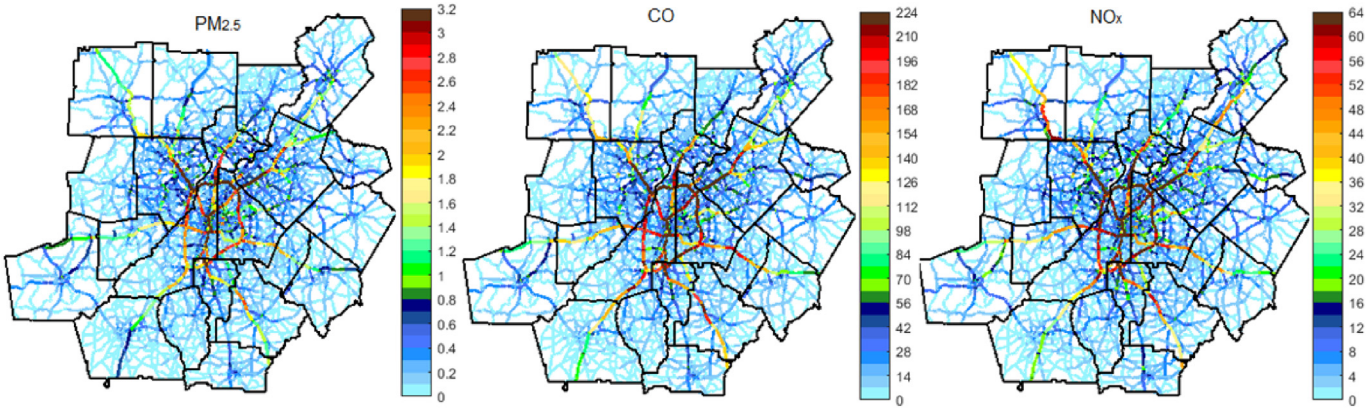

Fig. 1. Emissions of $PM_{2.5}$, CO, and NOx by mobile sources for 2010 in 20-county area in Atlanta (24 h average) (g/m/s).

Table 1
Stability categories for the meteorology conditions.

Parameter	Category	Range
Stability/Monin-Obukhov Length (m)	Unstable	−100 to 0
	Slightly Unstable	−500 to −100
	Neutral	<−500 or >500
	Slightly Stable	100 to 500
	Stable	0 to 100
Wind direction (degree)	N	0–45 & 315–360
	E	45–135
	S	135–225
	W	225–315
Wind speed (m/s)	Bin 1	$1 \leq n < 2$
	Bin 2	$2 \leq n < 4$
	Bin 3	$4 \leq n \leq 7$
	Bin 4	>7

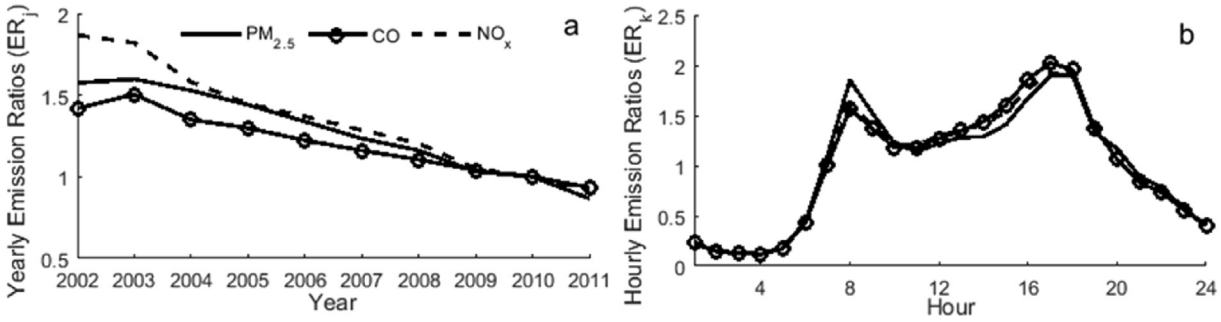

Fig. 2. Yearly (a) and diurnal (b) ratios of emissions. ER_j: total emissions of year j over total emissions of 2010; ER_k: total emissions of hour k over 24 h average total emissions.

hour are highly correlated with the 24 h average (R > 0.97 for CO and NO_x, R > 0.94 for $PM_{2.5}$), we further simplify the calculations by using 24 h averaged emissions as input in R-LINE for all hours and retrieve the emission trends using the ratios of the diurnal variation. Therefore, we define emission ratios for hour k (ER_k) as the total hourly emissions divided by the average of the 24 hourly emissions (Fig. 2b). Seasonality and weekly trends are not included in this study.

Overall, the annual average is calculated from the concentrations at the same location, adjusted for hourly and annual emissions as Equation (1), where k and m are the diurnal hour and meteorological category hour i is in.

$$C_j = ER_j * \frac{\sum_{i=1}^{H} ER_k * C_m}{\sum_{i=1}^{H} ER_k} \quad (1)$$

At each location, the annual average concentration for year j (C_j) is calculated from the annual average emission ratio ($\overline{ER_j}$) and an average over all hours (H) in each year with available meteorological data. The concentration of hour i out of H hours ($H \leq 8760$ or 8784 for leap years) in year j is calculated using the STAR bin concentration for bin m (C_m) that matches the meteorological condition of hour i, and weighted by the emission ratio k ($1 \leq k \leq 24$) that hour i happens in a day. Using our annual average approach (Fig. S1), we generated 10 years of annual average spatial fields of mobile source $PM_{2.5}$, CO, and NO_x in the Atlanta area. The method reduces the number of simulations by over 100 times, making the approach efficient and effective for both air quality management and exposure quantification purposes.

2.2. R-LINE model calibration

Annual CO and NO_x concentrations estimated by R-LINE are calibrated to ten years of monitor data at five locations for CO and seven for NO_x. Annual $PM_{2.5}$ mobile source impacts estimated by R-LINE are calibrated to CMB-GC mobile source impact estimates that are derived from observational data at three monitor sites using pre-determined source profiles. Both linear and log-transformed regressions are explored to optimize calibration, with regression parameters and their confidence intervals estimated using the "jackknife" resampling method (Sahinler and Topuz, 2007). That is, regression parameters are estimated with each available observation data point withheld one-at-a-time, resulting in 40 sets of results for CO, 63 for NO_x, and 30 for $PM_{2.5}$. Regression parameters are obtained by averaging results.

2.2.1. Ambient pollutant monitor data

$PM_{2.5}$ species concentrations were obtained from three sites: Yorkville (YRK), Jefferson Street (JST) and South DeKalb (SDK) (Fig. 3, Table S2). The YRK and JST sites are part of the Southeast Aerosol Research and Characterization network (SEARCH) (Hansen et al., 2003), and the SDK site is part of the Chemical Speciation Network (CSN) (Malm et al., 2011). These three sites also monitor CO and NO_x concentrations, along with additional two sites for CO and four additional sites for NO_x (Fig. 3). Two of the CO sites and two of the NO_x sites do not have data for all years. There are two YRK monitors for NO_x at the same location (within 10 m). The gas concentrations are obtained from U.S. EPA's Air Quality System (AQS) and SEARCH Network (Environmental Protection Agency; Hansen et al., 2003). Annual averages of 2002–2011 for each site are shown in Supplemental Tables S4 and S5 for CO and NO_x. YRK and Conyers are located in rural areas.

2.2.2. CMB-GC

The chemical mass balance model with gas constraints (CMB-GC) is a receptor model that modifies CMB with gas ratios (Marmur et al., 2005). CMB uses predetermined source profiles to identify the contribution from each source by using the species concentrations of $PM_{2.5}$. CMB-GC, previously referred as CMB-LGO (Marmur et al., 2005), requires species concentrations of $PM_{2.5}$ to identify the sources and contributions, and gas concentrations (e.g. CO, NO_x, and SO_2) to help separate source impacts. In Atlanta, only three sites, YRK, JST and SDK, measure $PM_{2.5}$ species concentrations.

2.3. Evaluation methods

Cross validation analysis is applied to evaluate the calibration models in two ways: leave-one-value-out and leave-one-site-out. The raw R-LINE estimates and the calibrated R-LINE estimates

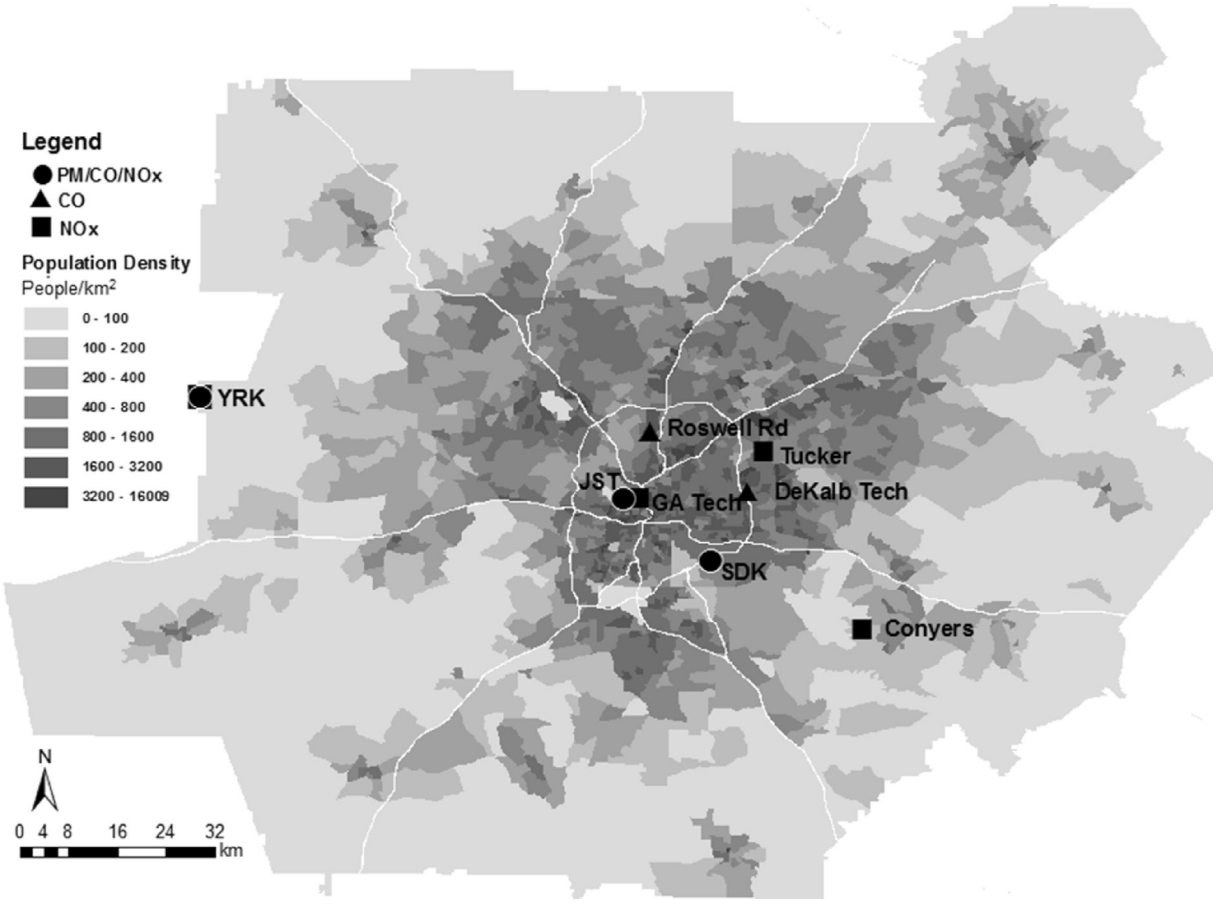

Fig. 3. Map of monitoring sites used in Atlanta with population density using 2010 census block data. White lines denote highways. There are two YRK sites: the SEARCH site monitors $PM_{2.5}$/CO/NO_x, and the AQS site monitors NO_x.

from cross validation analyses (referred as Estimate in the equations below) are compared with observations for CO and NO_x, and with CMB-GC estimates for $PM_{2.5}$ mobile source impacts, using normalized root mean square error (NRMSE) and normalized mean bias (NMB) metrics (Equations (2) and (3)). The leave-one-value-out approach provides 40 results for CO (available data in 10 years at 5 sites), 63 results for NO_x (available in 10 years at 7 sites), and 30 results for $PM_{2.5}$ (10 years and 3 sites). These results are used for estimating regression parameters for calibration, as already described, as well as for evaluating the calibration model performance. In the leave-one-site-out approach, one site is withheld (all ten years of data) and the sensitivity of calibration model results to the number of sites is assessed. For CO and NO_x, all monitors were withheld (one-at-a-time); for $PM_{2.5}$, only two of the three monitors were withheld, as accurate calibration requires at least one rural monitor.

$$NRMSE = \frac{1}{N}\sum_{m=1}^{N}\frac{\sqrt{\overline{(Estimate_m - OBS_m)^2}}}{\overline{OBS_m}} \quad (2)$$

$$NMB = \frac{1}{N}\sum_{m=1}^{N}\frac{\left(\overline{Estimate_m} - \overline{OBS_m}\right)}{\overline{OBS_m}} \quad (3)$$

2.4. Regional scale models

Calibrated R-LINE annual mean fields at 250 m resolution are up-scaled to coarser resolutions for comparison with results from previous studies derived using regional scale models. The regional scale models used are described here.

2.4.1. CMAQ-observation fusion method

The CMAQ model is a chemical transport model that simulates air quality, accounting for emissions, meteorology, chemical reactions, and physical transport (Byun et al., 1997). Friberg et al. (2016) developed a method that fused CMAQ simulation results and observation data to minimize bias and to optimize simulations of temporal and spatial variation. We compare 2002–2011 annual mean concentration fields of 1 h maximum CO and NO_x using the fused CMAQ-observation method at 12 km resolution (97 grid locations in study area) with the calibrated R-LINE results up-scaled to this resolution (i.e., averaging 48 × 48 values at 250 m resolution).

2.4.2. Integrated mobile source indicator method

The Integrated Mobile Source Indicator (IMSI) method is an approach that uses emission inventory information and concentrations of NO_x, CO, and EC to estimate the mobile source impacts on $PM_{2.5}$ (Pachon et al., 2012). The indicator is a weighted average of normalized concentrations of the three species, with the weighting determined by the ratios of mobile source emissions to total emissions for each species. The unitless indicator accounts for

the temporal and spatial variation of NO_x, CO, and EC concentrations. This unitless indicator is scaled to the CMB-GC mobile $PM_{2.5}$ source impacts obtained at three sites and multiple years (Table S3) by linear regression. The procedure is described in the Supplemental Information (Equation S(1)).

We generated 2008–2010 annual mean mobile source impact fields at a 4 km resolution for spatial comparison with the R-LINE mobile source $PM_{2.5}$ results using concentrations fields from the fused CMAQ-observation approach (Friberg et al., 2016) and emission weighting factors simulated by the Sparse Matrix Operator Kernel Emissions System (SMOKE) (Houyoux et al., 2000). The 4 km CMAQ data are available from the Hu et al. (Hu et al., 2010; Hu, 2014) study (4 km resolution data were not available for periods prior to 2008). Calibrated R-LINE results are up-scaled to 4 km resolution (i.e., averaging 16 × 16, 250 m resolution values).

3. Results and discussion

3.1. R-LINE model estimates

Annual average concentration fields of 24 h average $PM_{2.5}$, daily 1 h maximum CO, and NO_x concentrations were developed by R-LINE in metropolitan Atlanta for 2002 through 2011 (Fig. 4a–c, for 2011, Fig. S3 for other years). Estimated annual average concentrations decreased over time substantially at urban locations, with little change at rural site locations (Fig. S4, a to c).

The annual average approach is computationally efficient and reduces the impact of calm conditions. When calm conditions (wind speed < 1 m/s) are not reset, the calculated annual concentrations for all years increased by about 25%–30% for $PM_{2.5}$, and 28%–33% for CO and NO_x, averaged across the domain (Fig. S5). The largest relative impact of calm conditions occurs in rural areas, where $PM_{2.5}$ concentrations increases by about 4.5 times, and CO and NO_x concentrations increase by about 11 times (Fig. S6).

The adjustment of 24 h diurnal emission ratios reduces the annual averages. As meteorological conditions and diurnal traffic patterns are correlated, using daily average emissions without diurnal emission profile increase the concentrations by 60% for $PM_{2.5}$, 33% for 1 h maximum CO, and 30% for 1 h maximum NO_x averaged across the domain (Fig. S7). The highest impact of the diurnal emission adjustment occurs in the lower concentrations regions (Fig. S8). The impact is lower for the daily 1 h maximum concentrations than 24 h average concentrations. This is because the 24 h average concentrations are highly overestimated when the lower nighttime emissions are not accounted for and the atmosphere tends to be stable.

While the spatial fields of annual means look similar across years due to the largely static distribution of traffic emissions, some differences in these spatial fields due to meteorological variations were observed and varied by region. In the urban core, where population densities are mostly above 200 people/km^2 (Fig. 3) and the highest quartiles of concentrations are observed (Fig. S9), annual mean fields varied between years by up to 5%, 7%, and 7%, for $PM_{2.5}$, CO, and NO_x, respectively, based on the Pearson R^2 values for this quartile. The second and third quartiles of concentrations are in suburban areas with lower population density. Meteorological differences across years resulted in up to 81%, 67%, and 64% variations in the annual spatial patterns of the second quartile, and 63%, 71%, and 71% variations in the spatial patterns of the third quartile for $PM_{2.5}$, CO, and NO_x, respectively. For the lowest quartile concentrations which are in rural areas, up to 14%, 20, and 19% variations in the annual spatial patterns are attributed to meteorology for the three species. These results indicate that the change of spatial distribution in annual mean concentrations over years is greater in suburban areas than in urban and rural areas. This implies that the spatial distribution of pollutant concentrations in urban and rural areas is highly determined by traffic distribution; while in suburban area is highly influenced by meteorological impacts.

The maximum annual average concentrations from R-LINE model near roadways are very high. The maximum annual averages of mobile source $PM_{2.5}$, CO, and NO_x are observed in the downtown and midtown areas of Atlanta where two interstate highways (I-75 and I-85) are merged and the 2013 annual average daily traffic is

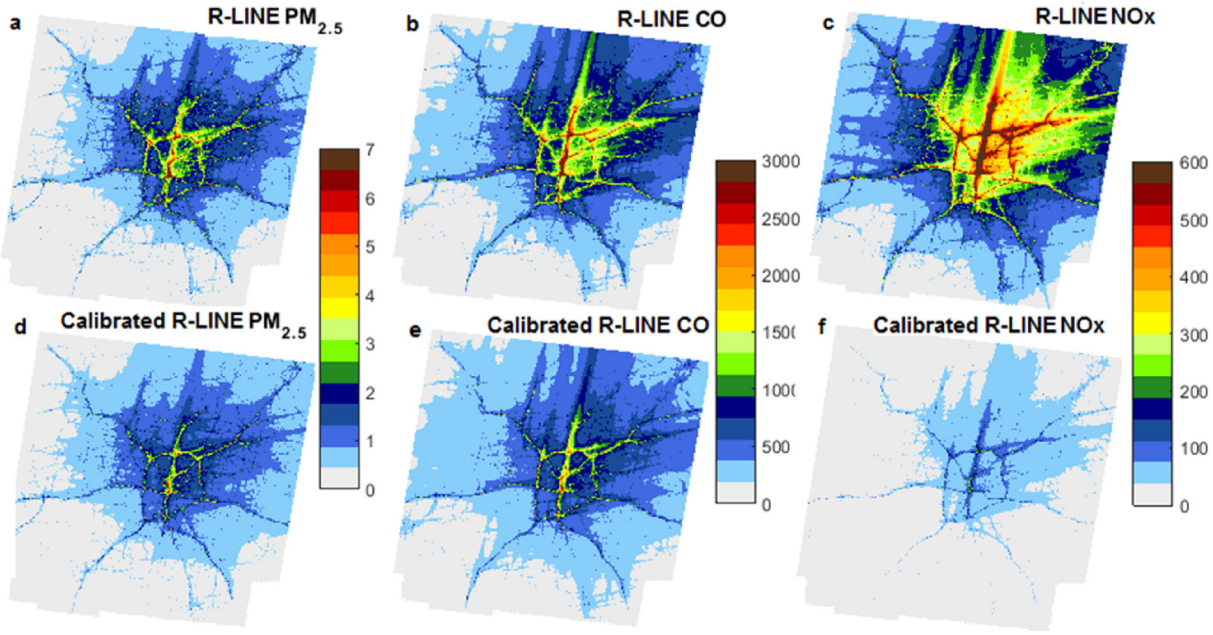

Fig. 4. Annual averages of R-LINE estimates by mobile sources in 2011. Panels a and d for $PM_{2.5}$ (μg/m^3), panels b and e for daily 1 h maximum CO (ppb), and panels c and f for daily 1 h maximum NO_x (ppb). $PM_{2.5}$ R-LINE results in panel d were calibrated on a log basis, whereas CO in panel e and NO_x R-LINE results in panel f were calibrated on a linear basis.

289,740 (Georgia Department of Transportation, 2013). Over the 10-year period, the maximum mobile impacts simulated by R-LINE ranged from 27.5 (2011) to 52.5 (2002) μg/m^3 for $PM_{2.5}$, 8140 (2008) to 13,141 (2002) ppb for CO, and 1683 (2011) to 3615 ppb (2002) for NO_x; within a 250 m distance, these peak concentrations drop dramatically. Near-roadway studies suggest that the peak R-LINE concentrations and steep near-road gradients are too high. Based on data from a recent near-roadway measurement study in Atlanta (Environmental Protection Agency), measurements of CO and NO_x were lower than R-LINE estimates by a factor of 3.1 and 7.4, respectively; more details are provided in SI Fig. S12 and Table S10.

3.2. R-LINE model calibration and evaluation

As 88% and 73% (averaged across the domain (Fig. S10)) of ground level CO and NO_x emissions, respectively, are estimated to be contributed by mobile sources, the annual spatial fields of mobile source contributed concentrations are directly compared with total ambient CO and NO_x observations. We compared the R-LINE derived mobile source $PM_{2.5}$ estimates, on the other hand, to CMB-GC estimated mobile source impacts of $PM_{2.5}$ based on observational data since a much smaller percentage of $PM_{2.5}$ is contributed directly by mobile sources.

We explore the relationships between R-LINE estimates at monitor locations and CO and NO_x measurements and CMB-GC estimates of $PM_{2.5}$ mobile source impacts using linear and log-transformed regressions (Fig. 5). The comparison indicates that the R-LINE model captures the trends at monitor locations well, with Pearson R^2 values over multiple years and locations for $PM_{2.5}$, CO, and NO_x of 0.72, 0.83, and 0.64, respectively, on a linear basis and 0.91, 0.91, and 0.89, respectively, on a log basis.

Simulated fields of all three species are biased high compared to observational data, indicating overestimation of the R-LINE model. Linear regression of R-LINE estimates and observational data (panels a–c) have slopes of 0.54, 0.69, and 0.30 for $PM_{2.5}$, CO, and NO_x, respectively, indicating higher simulated spatial gradients than observed. Several factors can lead to discrepancies between the R-LINE estimates at monitor locations and CO and NO_x measurements and CMB-GC estimates of $PM_{2.5}$ mobile source impacts. These include the formulation of the model, the properties of the pollutants, the impact from other sources, and the uncertainties in the models and data. The R-LINE model formulation does not include reaction and wet deposition. The R-LINE model generates least bias for CO as a primary pollutant gas with low reactivity and deposition loss. Wet deposition is a sink for mobile source $PM_{2.5}$ (Zhang et al., 2015), and NO_x is lost by reaction in the atmosphere. At the rural sites (YRK and Conyers), R-LINE estimated NO_x concentrations are much higher than observations. This may be due to the lack of sinks in R-LINE resulting in larger impacts from urban core emissions, and due to an over-estimation of modeled emissions (Anderson et al., 2014; Fujita et al., 2012; Liu and Frey, 2015). Moreover, there is a mismatch between the R-LINE estimates and the data used for calibration from direct measurements and from CMB-GC estimates. For CO and, to a lesser extent, NO_x, the observations include impacts of other sources, such as CO derived from oxidation of organics in the atmosphere, whereas the R-LINE estimates are derived entirely from traffic emissions. For $PM_{2.5}$, the CMB-GC estimates, while observation based, are prone to modeling uncertainties of about 45% of mobile source impacts on average based on a study at JST conducted from 1999 to 2004 (Balachandran et al., 2013); this uncertainty is due to uncertainties in measurements and specified source profiles and limitations in the calculation methodology such as number of sources.

Calibrating R-LINE estimates based on observations and models that use observational data can substantially improve exposure assessment and more accurately reflect mobile source impacts on pollutant concentrations for planning purposes. Here we use linear and log-transformed regression analyses (Fig. 5) to develop equations for calibrating R-LINE estimates to CO and NO_x measurements and CMB-GC $PM_{2.5}$ mobile source impacts using all available monitors from 2002 to 2011 in the domain. Error and bias for the raw R-LINE estimates and the calibrated R-LINE estimates are shown in Table 2. A discussion of results for each species follows.

3.2.1. $PM_{2.5}$

For mobile source $PM_{2.5}$, the log-transformed regression of the R-LINE estimates and CMB-GC estimates performed better than the linear regression (Table 2) using leave-one-value-out cross validation, with lower NRMSE and NMB (Table 2), and higher R^2 (Fig. 5 −0.91 for log regression versus 0.72 for linear regression). The slope of log-transformed regression is less than one, and the NMB of R-LINE estimates at all three sites are positive compared to CMB-GC results, indicating that calibration reduces near-roadway gradients. Therefore, the log-transformed regression was used to calibrate the R-LINE mobile source impacts of $PM_{2.5}$.

The calibrated R-LINE estimates are spatially more homogeneous than the raw R-LINE results, with the lower values increased slightly and the higher values decreased (Fig. 4d). The leave-one-value-out cross validation indicates that the calibration models are capable of estimating the mobile source impacts with lower NRMSE, 24% compared to 39% by R-LINE, and less NMB, 0.3% compared to 29% by R-LINE (Table 2).

However, with only three sites available for estimates of mobile source $PM_{2.5}$, one rural site and two urban sites, the impact of removing a site is substantial. In our leave-one-site-out evaluation, we only considered withholding one of the two urban monitors as the regression results are very poor without the rural monitor. Calibration with an urban monitor withheld resulted in higher NRMSE than the raw R-LINE data (49% versus 39%) and lower NMB (13% versus 29%). The higher NRMSE in the calibrated R-LINE results suggests that at least three monitors, spatially distributed, are needed to provide reliable calibration.

3.2.2. CO

For 1 h maximum CO, the log-transformed and linear regressions of the R-LINE estimates and observations performed similarly (Table 2). Linear regression yielded an intercept of 82 ppb (95% confidence interval as 81–83 ppb), which compares well with a U.S. background concentration estimated to as 40–200 ppb (Seinfeld and Pandis, 2012) and with background levels found at rural locations in the southeastern U.S (Blanchard et al., 2013). When the background of 82 ppb is removed from observations and the log regression is rerun, a slope of 1.007 (±0.04) is found, indicating that, when the background is removed, the linear and log-transformed relationships are effectively the same. Therefore, we opted to use a linear calibration equation.

Compared to the raw R-LINE estimates, the calibrated R-LINE estimates using the linear calibration are slightly higher in rural areas due to the addition of a background concentration of 82 ppb (Fig. 4e), and maximum concentrations decrease by about 30%. Linear calibration of the CO estimated NRMSE of 17%, compared to 33% by R-LINE, and NMB of 2%, compared to 22% by R-LINE.

Cross validation by withholding each monitor from the analysis yields smaller NRMSE and NMB, similar to the leave-one-value-out R-LINE results (Table 2). This suggests that the annual mean field estimated by R-LINE for 1 h maximum CO, calibrated with five CO monitors in the metropolitan Atlanta area, is weakly sensitive to the number of monitors. With the CO monitors covers rural, urban, suburban, and near road locations, the calibration model is able to captures the spatial distribution using the sufficient inputs. As a

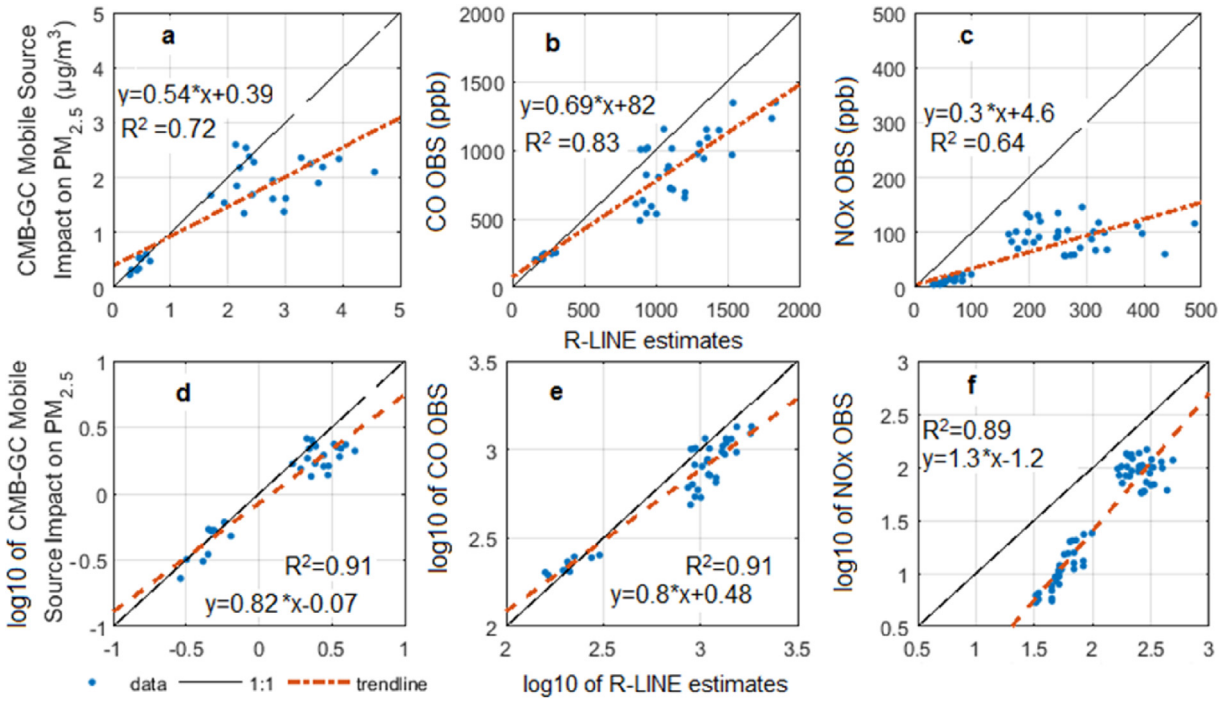

Fig. 5. Regressions between R-LINE estimates and CMB-GC estimates of mobile source $PM_{2.5}$ and observations for CO and NO_x, performed on a linear basis in the top row and log basis in bottom row.

result, the calibration model generates less errors and biases when monitors are more spatially distributed.

3.2.3. NO_x

For 1 h maximum NO_x, comparison of R-LINE estimates with observations indicates that R-LINE overestimates NO_x at both urban and rural locations. The raw R-LINE NRMSE is 326% and NMB is 303%. NO_x is most biased at rural sites, with NRMSE 510% and NMB 490% at YRK site, compared to 250% for NRMSE and 230% for NMB averaged across all urban sites. Log-transformed regression yields a slope of 1.3, resulting in larger near-road concentrations than calibration by linear regression. The near-zero intercept of the linear regression is consistent with a traffic dominated impact on NO_x. Therefore, we chose the linear regression for calibrating NO_x.

Compared to the raw R-LINE estimates, the distribution of results using linear calibration (Fig. 4f) shows a decrease of 59% at the lowest quartile, 64% at median, and 67% at top quartile. Linear calibration evaluated using the leave-one-value-out approach yields NRMSE of 70% compared to 326% by R-LINE, and NMB of 49% compared to 303% by R-LINE, substantially reducing the errors and biases.

Cross validation by withholding each of the six monitor locations one-by-one (two YRK sites withheld together) also shows lower NRMSE and NMB compared to R-LINE. This indicates the improvement by calibration over raw R-LINE results is only slightly sensitive to the number of monitor locations available for calibration in the case of NO_x with its six distinct monitor locations.

3.2.4. Model selection

Based on the discussion above, the equations shown in Table 3 were selected for calibration. For $PM_{2.5}$, the log-transformed linear regression is selected with slope of 0.818 (95% confidence intervals as 0.817 to 0.819 using the jackknife regression method) and intercept of 0.072 (confidence interval as 0.069 to 0.075). For CO, linear regression selected with a background of 82 ppb (confidence interval of 81–83 ppb), and slope of 0.688 (confidence interval of 0.687–0.689) as scaling factor of the spatial gradients. For NO_x, linear approach is selected, with spatial scaling factor of 0.301 (confidence interval as 0.300 to 0.302) and intercept of 4.6 (confidence interval as 4.5 to 4.7). Calibrated fields for 2011 are shown in Fig. 4d–f; calibrated fields for years 2002–2010 are shown in Supplemental Information (Fig. S11).

3.3. Comparison with regional scale model results

To assess consistency between the fine resolution R-LINE

Table 2
Error and bias from cross validation.

Regression		NRMSE			NMB		
		Raw R-LINE	Leave-one-value-out	Leave-one-site-out	Raw R-LINE	Leave-one-value-	Leave-one-site-out
$PM_{2.5}$	linear	39%	35%	50%	29%	13%	12%
	log		24%	49%		0.3%	13%
CO	linear	33%	17%	20%	22%	2%	1%
	log		16%	16%		−1%	1%
NO_x	linear	326%	70%	101%	303%	49%	69%
	log		44%	63%		15%	20%

Table 3
Selected models for calibrating R-LINE.

Species	Form	95% Confidence intervals of		Correlation coefficient
		Slope	Intercept	
$PM_{2.5}$	log10-transformed	0.818 ± 0.001	0.072 ± 0.003	0.95
1 h-max CO	linear	0.688 ± 0.001	82 ± 1	0.90
1 h-max NO_x	linear	0.301 ± 0.001	4.6 ± 0.1	0.80

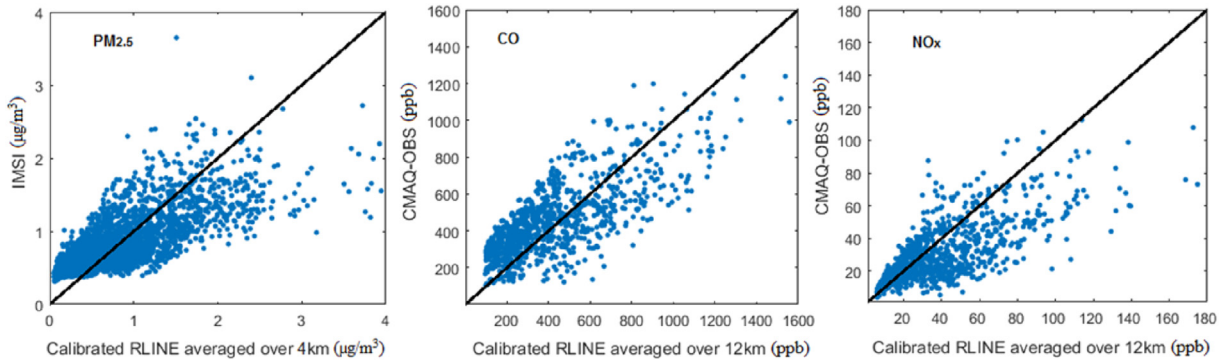

Fig. 6. Calibrated R-LINE results versus IMSI mobile source $PM_{2.5}$ estimates at 4 km resolution for 2008–2010 and versus CMAQ-observation fused CO and NO_x at 12 km resolution for 2002–2011.

modeling approach used here and regional scale approaches using coarser resolution chemical transport modeling, we compared calibrated R-LINE results aggregated to a 12 km resolution to correspond to CMAQ-observation fused estimates for CO and NO_x for 10 years (2002–2011), and aggregated to a 4 km resolution to correspond to IMSI mobile source impact fields for $PM_{2.5}$ for the three years 2008–2010, the time period for which data are available from other studies (Hu, 2014). The spatially averaged calibrated R-LINE estimates of CO and NO_x agree well with CMAQ-observation spatial distribution, with R^2 0.55 for CO, and 0.54 for NO_x, for $PM_{2.5}$ agree well with IMSI with R^2 0.53 (Fig. 6).

The comparisons in Fig. 6 are spatiotemporal, with 3 years and 873 locations for $PM_{2.5}$ and 10 years and 97 locations for CO and NO_x. The calibrated R-LINE $PM_{2.5}$ results approach zero at low concentrations whereas the IMSI results have a non-zero minimum. The IMSI minimum concentration is due to the inclusion of background CO and EC levels in the IMSI estimation; the R-LINE results include no background and no intercept was used in the $PM_{2.5}$ calibration.

3.4. Population-weighted concentration

To assess the impact of the fine resolution modeling on exposure estimates, we use 2010 census block data (Census Bureau, 2012), distributed to 250 m grid cells by weighting the population in each cell by area in the block, to estimate population-weighted concentration. Population at 250 m, 4 km and 12 km resolution are estimated and population-weighted spatial averages are obtained by equation (4).

$$\text{population weighted concentration} = \frac{\sum_{i}^{N} conc_i \times population_i}{\sum_{i}^{N} population_i} \quad (4)$$

Here, N is the number of 250 m grid cells (235,296). Population-weighted annual mean concentration estimates using raw R-LINE, calibrated R-LINE, and regional scale model fields were calculated for the three pollutants (Table 4 for 2010 and Table S9 for all years). The mobile contributed concentrations based on calibrated R-LINE and IMSI are 11% and 9% of the concentrations based on total $PM_{2.5}$ concentrations using a CMAQ-OBS data fusion approach at 4 km resolution in 2010 (12.8 μg/m^3). Over the 10-year period (2002–2011), calibration reduced the R-LINE-based population-weighted concentration by 28%–36% for mobile contributed $PM_{2.5}$, by 24%–30% for CO, and by 202%–216% for NO_x (Table S9). Even after calibration, the population-weighted concentration based on R-LINE is greater than the population-weighted concentration based on regional scale modeling, possibly due to the coarse resolution of the regional scale modeling underestimating urban exposures. On the other hand, exposure estimates based on central site data alone, such as the CMB-GC mobile source impact estimates and observations of CO and NO_x at the Atlanta central monitor JST, are higher than the population-weighted concentrations based on calibrated R-LINE, on average by 12% for $PM_{2.5}$, by 60% for NO_x, and by 21% for CO. This suggests that the fine scale spatial distributions of traffic-related pollution and population are correlated and likely results in higher exposures than predicted by regional scale models

Table 4
Population-weighted concentration in 2010 by the raw R-LINE, calibrated R-LINE, and regional scale models.

	R-LINE	Calibrated R-LINE	IMSI/CMAQ-OBS
$PM_{2.5}$ mobile source impact (μg/m^3)	1.88	1.37	1.11
CO (ppb)	733	588	295
NO_x (ppb)	148	49	31

and lower exposures than predicted by central site monitors.

3.5. Limitations

The calibrated R-LINE approach developed here for estimating annual average mobile source pollutant concentration fields at fine resolution is computationally efficient and consistent with available observational data. However, there are several limitations to the approach.

One limitation of our approach is use of the STAR method for categorizing meteorological parameters in the development of R-LINE annual average fields. For example, in this study we divided the wind direction into four bins, which can lead to substantial spatial discrepancies. Finer categorization can help reduce these errors, but at the cost of computational efficiency. Evaluation of the STAR method, coupled with the treatment of calm conditions and the use of average diurnal emission trends described in this work, could be improved with better spatial coverage of observations to better characterize the tradeoffs between computational efficiency and accurate simulations.

A second limitation of the calibrated R-LINE approach is its dependence on available monitor data in developing the calibration models. Although there may be a sufficient number of years available, a study area may not have a sufficient number of monitors to provide adequate spatial coverage. In this study of metropolitan Atlanta, the three monitors with speciated $PM_{2.5}$ were marginally sufficient to calibrate mobile source $PM_{2.5}$ R-LINE estimates, reducing bias but increasing error. For CO and NO_x, the numbers of monitors available (five and seven, respectively) were sufficient to reduce bias and error in the R-LINE annual estimates based on cross-validation results. The spatial distribution of monitors used for calibration is also an important factor in calibration of R-LINE estimates.

The use of CMB-GC to estimate mobile source $PM_{2.5}$ is another limitation of the calibrated R-LINE approach. As there is no direct measurement of mobile source impacts and mobile sources contribute only a small portion of total $PM_{2.5}$, R-LINE $PM_{2.5}$ calibration is based on CMB-GC source apportionment modeling that uses speciated $PM_{2.5}$ data. Uncertainties in source apportionment modeling are large, as evidenced by the range of results obtained by applying different methods (Balachandran et al., 2013). Moreover, the availability of speciated $PM_{2.5}$ measurements is limited over time and space. One solution is to compare the mobile source impacts to the more commonly measured total $PM_{2.5}$ concentrations assuming a spatial homogeneous contribution from all other sources in the domain, as applied in D'Onofrio et al. (2016).

While R-LINE can be used to estimate mobile source pollutant concentrations at very fine resolution, the accuracy of results will be limited by the use of the STAR approach developed for computational efficiency as well as the emission data used for road links. Calibration can reduce biases in near-road gradients in the R-LINE estimates, but long-term (i.e. five or more years) monitoring at multiple sites that are spatially distributed (e.g. at least one urban, suburban and rural monitor) are needed to develop the regression models. Finally, attention must be paid to the potential mismatch of R-LINE estimates of pollutant concentrations, which are from mobile sources only, and pollutant measurements used for calibration, which are from all sources.

4. Conclusion

Calibrated R-LINE modeling provides high-resolution annual mean concentration fields useful for air quality planning and long-term exposure studies. In particular, we extended the STAR approach for the treatment of calm meteorological conditions, diurnal emission adjustment, and calibration to observational data. In the application of R-LINE with a ten-year period in the metropolitan Atlanta region, the annual average approach reduces computation time, and the treatment of calm conditions and application of diurnal emission ratios in calculating that annual averages reduce the estimates substantially. The calibration method reduces bias and NRMSE. The calibration model requires at least three spatially distributed sites; otherwise it becomes sensitive to the change of sites used. The calibrated R-LINE results at the fine resolution present higher population exposures than estimated by calibrated regional scale models. This study for the spatial information help improve and understand the infrastructure project planning. The approach has been applied to scale simulated concentrations for air quality analyses by the ARC (D'Onofrio et al., 2016). The results are also being used for fine scaled health analysis.

Acknowledgement

This study was conducted as part of the Southeastern Center for Air Pollution and Epidemiology (SCAPE) supported by U.S. EPA under Grant Number R834799. Its contents are solely the responsibility of the grantee and do not necessarily represent the official views of the U.S. EPA. Further, U.S. EPA does not endorse the purchase of any commercial products or services mentioned in the publication. We would like to acknowledge the measurement networks IMPROVE, CSN, and SEARCH. We acknowledge Yongtao Hu for providing the data for comparison in our modeling process.

Appendix A. Supplementary data

Supplementary data related to this article can be found at http://dx.doi.org/10.1016/j.atmosenv.2016.10.015.

References

Anderson, D.C., Loughner, C.P., Diskin, G., Weinheimer, A., Canty, T.P., Salawitch, R.J., Worden, H.M., Fried, A., Mikoviny, T., Wisthaler, A., Dickerson, R.R., 2014. Measured and modeled CO and NOy in DISCOVER-AQ: an evaluation of emissions and chemistry over the eastern US. Atmos. Environ. 96, 78–87.

Arain, M.A., Blair, R., Finkelstein, N., Brook, J.R., Sahsuvaroglu, T., Beckerman, B., Zhang, L., Jerrett, M., 2007. The use of wind fields in a land use regression model to predict air pollution concentrations for health exposure studies. Atmos. Environ. 41, 3453–3464.

Balachandran, S., Chang, H.H., Pachon, J.E., Holmes, H.A., Mulholland, J.A., Russell, A.G., 2013. Bayesian-based ensemble source apportionment of PM2.5. Environ. Sci. Technol. 47, 13511–13518.

Baldassarre, G., Pozzoli, L., Schmidt, C.C., Unal, A., Kindap, T., Menzel, W.P., Whitburn, S., Coheur, P.F., Kavgaci, A., Kaiser, J.W., 2015. Using SEVIRI fire observations to drive smoke plumes in the CMAQ air quality model: a case study over Antalya in 2008. Atmos. Chem. Phys. 15, 8539–8558.

Beckerman, B.S., Jerrett, M., Serre, M., Martin, R.V., Lee, S.J., van Donkelaar, A., Ross, Z., Su, J., Burnett, R.T., 2013. A hybrid approach to estimating National scale spatiotemporal variability of PM2.5 in the contiguous United States. Environ. Sci. Technol. 47, 7233–7241.

Blanchard, C.L., Hidy, G.M., Tanenbaum, S., Edgerton, E.S., Hartsell, B.E., 2013. The Southeastern Aerosol Research and Characterization (SEARCH) study: temporal trends in gas and PM concentrations and composition, 1999-2010. J. Air Waste Manag. 63, 247–259.

Bowers, J., Bjorklund, J., Cheney, C., Schewe, G.J., 1980. Industrial Source Complex (ISC) Dispersion Model User's Guide. US Environmental Protection Agency, Office of Air Quality Planning and Standards.

Brook, R.D., Rajagopalan, S., Pope, C.A., Brook, J.R., Bhatnagar, A., Diez-Roux, A.V., Holguin, F., Hong, Y.L., Luepker, R.V., Mittleman, M.A., Peters, A., Siscovick, D., Smith, S.C., Whitsel, L., Kaufman, J.D., Epidemiol, A.H.A.C., Dis, C.K.C., Metab, C.N.P.A., 2010. Particulate matter air pollution and cardiovascular disease an update to the scientific statement from the American Heart association. Circulation 121, 2331–2378.

Byun, D., Young, J., Gipson, G., Godowitch, J., Binkowski, F., 1997. Description of the Models-3 Community Multiscale Air Quality(CMAQ) Modeling System.

Census Bureau, U.S, 2012. Summary Population and Housing Characteristics 2010 Census of Population and Housing (census.gov).

Chang, S.Y., Vizuete, W., Valencia, A., Naess, B., Isakov, V., Palma, T., Breen, M., Arunachalam, S., 2015. A modeling framework for characterizing near-road air pollutant concentration at community scales. Sci. Total Environ. 538, 905–921.

Chen, H., Goldberg, M.S., Burnett, R.T., Jerrett, M., Wheeler, A.J., Villeneuve, P.J., 2013. Long-term exposure to traffic-related air pollution and cardiovascular mortality. Epidemiology 24, 35–43.
Cimorelli, A.J., Perry, S.G., Venkatram, A., Weil, J.C., Paine, R.J., Wilson, R.B., Lee, R.F., Peters, W.D., Brode, R.W., 2005. AERMOD: a dispersion model for industrial source applications. Part I: general model formulation and boundary layer characterization. J. Appl. Meteorol. 44, 682–693.
Crooks, J.L., Ozkaynak, H., 2014. Simultaneous statistical bias correction of multiple PM2.5 species from a regional photochemical grid model. Atmos. Environ. 95, 126–141.
D'Onofrio, D., Kim, B., Kim, Y., Kim, K., 2016. Atlanta Roadside Emissions Exposure Study – Methodology & Project Overview. http://www.atlantaregional.com/environment/air/arees-near-road-emissions.
Environmental Protection Agency, U.S., Air Quality System Data Mart [internet database] available at http://www.epa.gov/ttn/airs/aqsdatamart.
Environmental Protection Agency, U.S, 1997. The STability ARray Program. In: https://www3.epa.gov/scram001/metobsdata_procaccprogs.htm.
Environmental Protection Agency, U.S, 2000. Meteorological Monitoring Guidance for Regulatory Modeling Applications. EPA.
Environmental Protection Agency, U.S, 2004a. EPA-CMB8.2 Usear's Manual.
Environmental Protection Agency, U.S, 2004b. User's Guide for the AERMOD Meteorological Preprocessor (AERMET).
Environmental Protection Agency, U.S, 2009. Integrated Science Assessment for Particulate Matter.
Environmental Protection Agency, U.S, 2011. Annual Data Summary Report for the Chemical Speciation of PM2.5 Filter Samples Project.
Environmental Protection Agency, U.S, 2012. Motor Vehicle Emission Simulator (MOVES) User Guide for MOVES2010b.
Environmental Protection Agency, U.S, 2013. User's Guide for R-LINE Model Version 1.2 a Research LINE Source Model for Near-surface Releases.
Environmental Protection Agency, U.S, 2015. AERMINUTE User's Guide.
Friberg, M.D., Zhai, X.D., Holmes, H., Chang, H.H., Strickland, M., Sarnat, S.E., Tolbert, P.E., Russell, A.G., Mulholland, J.A., 2016. Method for fusing observational data and chemical transport model simulations to estimate spatiotemporally-resolved ambient air pollution. Environ. Sci. Technol. 50, 3695–3705.
Fujita, E.M., Campbell, D.E., Zielinska, B., Chow, J.C., Lindhjem, C.E., DenBleyker, A., Bishop, G.A., Schuchmann, B.G., Stedman, D.H., Lawson, D.R., 2012. Comparison of the MOVES2010a, MOBILE6.2, and EMFAC2007 mobile source emission models with on-road traffic tunnel and remote sensing measurements. J. Air Waste Manag. 62, 1134–1149.
Gauderman, W.J., Vora, H., McConnell, R., Berhane, K., Gilliland, F., Thomas, D., Lurmann, F., Avol, E., Kunzli, N., Jerrett, M., Peters, J., 2007. Effect of exposure to traffic on lung development from 10 to 18 years of age: a cohort study. Lancet 369, 571–577.
Georgia Department of Transportation, U.S., 2013. http://www.dot.ga.gov/DriveSmart/MapsData/Documents/Statewide/TrafficFlowMap_Interstate_AADT.pdf.
Gulliver, J., Briggs, D., 2011. STEMS-Air: a simple GIS-based air pollution dispersion model for city-wide exposure assessment. Sci. Total Environ. 409, 2419–2429.
Hankey, S., Marshall, J.D., 2015. Land use regression models of on-road particulate air pollution (particle number, black carbon, PM2.5, particle size) using mobile monitoring. Environ. Sci. Technol. 49, 9194–9202.
Hansen, D.A., Edgerton, E.S., Hartsell, B.E., Jansen, J.J., Kandasamy, N., Hidy, G.M., Blanchard, C.L., 2003. The southeastern aerosol research and characterization study: Part 1-overview. J. Air Waste Manag. 53, 1460–1471.
Hoek, G., Beelen, R., de Hoogh, K., Vienneau, D., Gulliver, J., Fischer, P., Briggs, D., 2008. A review of land-use regression models to assess spatial variation of outdoor air pollution. Atmos. Environ. 42, 7561–7578.
Houyoux, M., Vukovich, J., Brandmeyer, J., Seppanen, C., Holland, A., 2000. Sparse Matrix Operator Kernel Emissions Modeling System-smoke User Manual (Prepared by MCNC-North Carolina Supercomputing Center, Environmental Programs, Research Triangle Park, NC).
Hu, Y., 2014. HiRes2 Air Quality & Source Impacts Forecasting for Georgia. https://forecast.ce.gatech.edu/hires_about.php.
Hu, Y., Chang, M.E., Russell, A.G., Odman, M.T., 2010. Using synoptic classification to evaluate an operational air quality forecasting system in Atlanta. Atmos. Pollut. Res. 1, 280–287.
Ivey, C.E., Holmes, H.A., Hu, Y.T., Mulholland, J.A., Russell, A.G., 2015. Development of PM2.5 source impact spatial fields using a hybrid source apportionment air quality model. Geosci. Model Dev. 8, 2153–2165.
Jerrett, M., Arain, A., Kanaroglou, P., Beckerman, B., Potoglou, D., Sahsuvaroglu, T., Morrison, J., Giovis, C., 2005. A review and evaluation of intraurban air pollution exposure models. J. Expo. Anal. Env. Epidemiol. 15, 185–204.
Lena, T.S., Ochieng, V., Carter, M., Holguin-Veras, J., Kinney, P.L., 2001. Elemental carbon and PM2.5 levels in an urban community heavily impacted by truck traffic. Epidemiology 12. S38–S38.
Lim, S.S., Vos, T., Flaxman, A.D., Danaei, G., Shibuya, K., Adair-Rohani, H., Amann, M., Anderson, H.R., Andrews, K.G., Aryee, M., Atkinson, C., Bacchus, L.J., Bahalim, A.N., Balakrishnan, K., Balmes, J., Barker-Collo, S., Baxter, A., Bell, M.L., Blore, J.D., Blyth, F., Bonner, C., Borges, G., Bourne, R., Boussinesq, M., Brauer, M., Brooks, P., Bruce, N.G., Brunekreef, B., Bryan-Hancock, C., Bucello, C., Buchbinder, R., Bull, F., Burnett, R.T., Byers, T.E., Calabria, B., Carapetis, J., Carnahan, E., Chafe, Z., Charlson, F., Chen, H.L., Chen, J.S., Cheng, A.T.A., Child, J.C., Cohen, A., Colson, K.E., Cowie, B.C., Darby, S., Darling, S., Davis, A., Degenhardt, L., Dentener, F., Des Jarlais, D.C., Devries, K., Dherani, M., Ding, E.L., Dorsey, E.R., Driscoll, T., Edmond, K., Ali, S.E., Engell, R.E., Erwin, P.J., Fahimi, S., Falder, G., Farzadfar, F., Ferrari, A., Finucane, M.M., Flaxman, S., Fowkes, F.G.R., Freedman, G., Freeman, M.K., Gakidou, E., Ghosh, S., Giovannucci, E., Gmel, G., Graham, K., Grainger, R., Grant, B., Gunnell, D., Gutierrez, H.R., Hall, W., Hoek, H.W., Hogan, A., Hosgood, H.D., Hoy, D., Hu, H., Hubbell, B.J., Hutchings, S.J., Ibeanusi, S.E., Jacklyn, G.L., Jasrasaria, R., Jonas, J.B., Kan, H.D., Kanis, J.A., Kassebaum, N., Kawakami, N., Khang, Y.H., Khatibzadeh, S., Khoo, J.P., Kok, C., Laden, F., Lalloo, R., Lan, Q., Lathlean, T., Leasher, J.L., Leigh, J., Li, Y., Lin, J.K., Lipshultz, S.E., London, S., Lozano, R., Lu, Y., Mak, J., Malekzadeh, R., Mallinger, L., Marcenes, W., March, L., Marks, R., Martin, R., McGale, P., McGrath, J., Mehta, S., Mensah, G.A., Merriman, T.R., Micha, R., Michaud, C., Mishra, V., Hanafiah, K.M., Mokdad, A.A., Morawska, L., Mozaffarian, D., Murphy, T., Naghavi, M., Neal, B., Nelson, P.K., Nolla, J.M., Norman, R., Olives, C., Omer, S.B., Orchard, J., Osborne, R., Ostro, B., Page, A., Pandey, K.D., Parry, C.D.H., Passmore, E., Patra, J., Pearce, N., Pelizzari, P.M., Petzold, M., Phillips, M.R., Pope, D., Pope, C.A., Powles, J., Rao, M., Razavi, H., Rehfuess, E.A., Rehm, J.T., Ritz, B., Rivara, F.P., Roberts, T., Robinson, C., Rodriguez-Portales, J.A., Romieu, I., Room, R., Rosenfeld, L.C., Roy, A., Rushton, L., Salomon, J.A., Sampson, U., Sanchez-Riera, L., Sanman, E., Sapkota, A., Seedat, S., Shi, P.L., Shield, K., Shivakoti, R., Singh, G.M., Sleet, D.A., Smith, E., Smith, K.R., Stapelberg, N.J.C., Steenland, K., Stockl, H., Stovner, L.J., Straif, K., Straney, L., Thurston, G.D., Tran, J.H., Van Dingenen, R., van Donkelaar, A., Veerman, J.L., Vijayakumar, L., Weintraub, R., Weissman, M.M., White, R.A., Whiteford, H., Wiersma, S.T., Wilkinson, J.D., Williams, H.C., Williams, W., Wilson, N., Woolf, A.D., Yip, P., Zielinski, J.M., Lopez, A.D., Murray, C.J.L., Ezzati, M., 2012. A comparative risk assessment of burden of disease and injury attributable to 67 risk factors and risk factor clusters in 21 regions, 1990-2010: a systematic analysis for the Global Burden of Disease Study 2010. Lancet 380, 2224–2260.
Liu, B., Frey, H.C., 2015. Variability in light-duty gasoline vehicle emission factors from trip-based real-world measurements. Environ. Sci. Technol. 49, 12525–12534.
Liu, X.H., Zhang, Y., Cheng, S.H., Xing, J., Zhang, Q.A., Streets, D.G., Jang, C., Wang, W.X., Hao, J.M., 2010. Understanding of regional air pollution over China using CMAQ, part I performance evaluation and seasonal variation. Atmos. Environ. 44, 2415–2426.
Lv, B.L., Hu, Y.T., Chang, H.H., Russell, A.G., Bai, Y.Q., 2016. Improving the accuracy of daily PM2.5 distributions derived from the fusion of ground-level measurements with aerosol optical depth observations, a case study in North China. Environ. Sci. Technol. 50, 4752–4759.
Malm, W.C., Schichtel, B.A., Pitchford, M.L., 2011. Uncertainties in PM2.5 gravimetric and speciation measurements and what we can learn from them. J. Air Waste Manag. Assoc. 61, 1131–1149.
Marmur, A., Unal, A., Mulholland, J.A., Russell, A.G., 2005. Optimization-based source apportionment of PM2.5 incorporating gas-to-particle ratios. Environ. Sci. Technol. 39, 3245–3254.
Nordling, E., Berglind, N., Melen, E., Emenius, G., Hallberg, J., Nyberg, F., Pershagen, G., Svartengren, M., Wickman, M., Bellander, T., 2008. Traffic-related air pollution and childhood respiratory symptoms, function and allergies. Epidemiology 19, 401–408.
Pachon, J.E., Balachandran, S., Hu, Y.T., Mulholland, J.A., Darrow, L.A., Sarnat, J.A., Tolbert, P.E., Russell, A.G., 2012. Development of outcome-based, multipollutant mobile source indicators. J. Air Waste Manag. 62, 431–442.
Parrish, D.D., 2006. Critical evaluation of US on-road vehicle emission inventories. Atmos. Environ. 40, 2288–2300.
Reche, C., Querol, X., Alastuey, A., Viana, M., Pey, J., Moreno, T., Rodriguez, S., Gonzalez, Y., Fernandez-Camacho, R., de la Campa, A.M.S., de la Rosa, J., Dall'Osto, M., Prevot, A.S.H., Hueglin, C., Harrison, R.M., Quincey, P., 2011. New considerations for PM, Black Carbon and particle number concentration for air quality monitoring across different European cities. Atmos. Chem. Phys. 11, 6207–6227.
Rowangould, G.M., 2013. A census of the US near-roadway population: public health and environmental justice considerations. Transp. Res. D. Transp. Environ. 25, 59–67.
Sahinler, S., Topuz, D., 2007. Bootstrap and jackknife resampling algorithms for estimation of regression parameters. J. Appl. Quant. Methods 2, 188–199.
Seinfeld, J.H., Pandis, S.N., 2012. Atmospheric Chemistry and Physics: from Air Pollution to Climate Change. John Wiley & Sons.
Snyder, M.G., Venkatram, A., Heist, D.K., Perry, S.G., Petersen, W.B., Isakov, V., 2013. RLINE: a line source dispersion model for near-surface releases. Atmos. Environ. 77, 748–756.
United States, U., 1990. An Act to Amend the Clean Air Act to Provide for Attainment and Maintenance of Health Protective National Ambient Air Quality Standards, and for Other Purposes. US Government Printing Office.
Venkatram, A., Isakov, V., Yuan, J., Pankratz, D., 2004. Modeling dispersion at distances of meters from urban sources. Atmos. Environ. 38, 4633–4641.
Venkatram, A., Isakov, V., Thoma, E., Baldauf, R., 2007. Analysis of air quality data near roadways using a dispersion model. Atmos. Environ. 41, 9481–9497.
Venkatram, A., Snyder, M.G., Heist, D.K., Perry, S.G., Petersen, W.B., Isakov, V., 2013. Re-formulation of plume spread for near-surface dispersion. Atmos. Environ. 77, 846–855.
Wang, X., Zhang, Y., Hu, Y., Zhou, W., Lu, K., Zhong, L., Zeng, L., Shao, M., Hu, M., Russell, A.G., 2010. Process analysis and sensitivity study of regional ozone formation over the Pearl River Delta, China, during the PRIDE-PRD2004 campaign using the Community Multiscale Air Quality modeling system.

Atmos. Chem. Phys. 10, 4423–4437.
Wang, M., Sampson, P.D., Hu, J.L., Kleeman, M., Keller, J.P., Olives, C., Szpiro, A.A., Vedal, S., Kaufman, J.D., 2016. Combining land-use regression and chemical transport modeling in a spatiotemporal geostatistical model for ozone and PM2.5. Environ. Sci. Technol. 50, 5111–5118.
Wilton, D., Szpiro, A., Gould, T., Larson, T., 2010. Improving spatial concentration estimates for nitrogen oxides using a hybrid meteorological dispersion/land use regression model in Los Angeles, CA and Seattle, WA. Sci. Total Environ. 408, 1120–1130.
Zhang, R.Y., Wang, G.H., Guo, S., Zarnora, M.L., Ying, Q., Lin, Y., Wang, W.G., Hu, M., Wang, Y., 2015. Formation of urban fine particulate matter. Chem. Rev. 115, 3803–3855.